Three-dimensional spheroids of mesenchymal stem/stromal cells promote osteogenesis by activating stemness and Wnt/β-catenin

Ayaka Imamura[1, 2], Hiroshi Kajiya[1, 3*], Seiichi Fujisaki[1,4], Munehisa Maeshiba[1,4], Tsukasa Yanagi[4], Hiroshi Kojima[2], and Jun Ohno[1]

[1]Research Centre for Regenerative Medicine, Fukuoka Dental College, 2-15-1Tamura, Fukuoka, Japan.

[2]Department of Oral Growth and Development, Fukuoka Dental College, 2-15-1Tamura, Fukuoka, Japan.

[3]Department of Physiological Science and Molecular Biology, Fukuoka Dental College, 2-15-1Tamura, Fukuoka, Japan.

[4]Department of Oral Rehabilitation, Fukuoka Dental College, 2-15-1Tamura, Fukuoka, Japan.

[*]**Corresponding author:**

Hiroshi Kajiya, Ph.D., Department of Physiological Science and Molecular Biology, Fukuoka Dental College, Tamura 2-15-1, Sawara-ku, Fukuoka 8140193, Japan

Tel: +81-92-801-0411 ext. 660

Fax: +81-92-801-4909

E-mail: kajiya@college.fdcnet.ac.jp

Abstract

Mesenchymal stem/stromal cells (MSCs) are multipotent and self-renewal cells that are widely used in regenerative medicine. The culture of three-dimensional (3D) spheroid MSCs more accurately mimics the biological microenvironment. However, it is unclear which key molecules are responsible for the cell fate control of MSCs during 3D spheroid formation and their impact on the functional characteristics of these stem cells. Furthermore, it remains unclear what effects 3D spheroid MSC transplantation has on new bone formation compared with that of 2D monolayer MSCs. We assessed whether the osteogenerative potential of 3D spheroid MSCs is greater than that of 2D monolayer MSCs *in vitro*. In addition, to elucidate the ability of 3D spheroid MSCs to regenerate bone, we examined the effects of transplanting wild-type (WT) or knockout (KO) spheroid MSCs on new bone formation in mice calvarial defect model *in vitro*.

The 3D spheroid MSC culture dramatically upregulated into stemness markers compared with the 2D monolayer MSC culture. In contrast, BMP-2 significantly increased the osteogenesis-related molecules in the 3D spheroid MSCs but, in turn, downregulated the stemness markers. BMP-2 activated Smad1/5 together with Wnt/β-catenin in 3D spheroid MSCs. Transplantation of these MSCs into aged mice with calvarial defects promoted new bone formation compared with that of 2D monolayer MSCs. In contrast, transplantation of 3D or 2D β-catenin knockout MSCs induced little new bone formation. The 3D spheroid MSC culture had higher stemness compared with the 2D monolayer MSC culture. The culture of 3D spheroid MSCs rapidly promoted osteoblastogenesis and bone formation through synergistic activation of the Wnt/β-catenin pathway *in vitro*. The transformation of 3D spheroid, but not 2D monolayer, MSCs promoted new bone regeneration *in vivo*.

These results indicate that transplantation of 3D spheroid MSCs in regeneration therapy contributes to a shorter regenerative healing process, including new bone formation.

Key words: Bone regeneration, Mesenchymal stem/stromal cells, Three dimension spheroid, Wnt/beta-catenin, stemness

1. Introduction

Mesenchymal stem/stromal cells (MSCs) are multipotent somatic stem cells that can differentiate into a variety of mesodermal cells, such as osteoblasts, chondrocytes, myocytes, and adipocytes [1]. Recent studies have demonstrated that cell engineering has been assessed in clinical trials using MSCs [2,3]. Furthermore, MSCs represent unique opportunities in cellular therapy owing to their ability to stimulate the regeneration of damaged tissues and organs.

Because of ease of use, two-dimensional (2D) monolayer conditions have been used as a standard technique in traditional cultures; however, these present a highly artificial and less physiological environment because some *in vitro* characteristics and traits are lost or compromised, such as self-renewal, replication, colony-forming efficiency, and differentiation capacity [4,5]. In contrast, three-dimensional (3D) spheroid cultures are regarded as more physiologically similar to these characteristics, which are then better preserved [6]. Furthermore, *in vitro* 3D spheroids have been used in the field of stem cell research [7], and an organoid culture shows that these stem cells exhibit better tissue-specific function to faithfully recapitulate the *in vivo* tissue development and regenerative processes [8]. Thus, the potential for osteogenesis differentiation using 3D spheroid MSCs is greater in bone-regenerative medicine. However, it is unclear about 3D spheroid MSCs may promote osteogenesis compare to 2D monolayer MSCs.

Accordingly, an increasing number of studies have employed spheroid aggregates of cultured MSCs and have found distinctive patterns of gene expression, increases in cytokine secretion, or multilineage differentiation compared with those of a 2D monolayer MSC culture [9]. Despite the increasing interest in 3D spheroid MSCs, it is unclear which key molecules are responsible for the cell fate control of MSCs during 3D spheroid formation and their impact on the functional characteristics of these stem cells. Furthermore, it remains

unclear what effects 3D spheroid MSC transplantation has on new bone formation compared with that of 2D monolayer MSCs.

In the present study, we assessed whether the osteogenerative potential of 3D spheroid MSCs is greater than that of 2D monolayer MSCs *in vitro*. In addition, to elucidate the ability of 3D MSCs to regenerate bone, we examined the effects of transplanting wild-type (WT) or knockout (KO) spheroid MSCs on new bone formation in an aged mice calvarial defect model *in vitro*.

2. Materials and Methods

2.1. Cell culture

Mouse bone marrow stromal precursor D1 ORL UVA cells (ATCC® CRL-12424 Manassas, VA, USA) were cultured in D-MEM (Fuji Film Wako, Japan) containing 10% FBS (Sigma-Aldrich Co., St. Louis, MO, USA) at 37 °C and 5% CO_2. The 3D MSCs formation was used for generation of spheroid MSCs as described by Itaka [10]. MSCs (4×10^5 cells/ml) were added to Cell able® low cell binding plates (Toyo Gosei, Tokyo, Japan) and incubated up to 48 h. After re-plated 3D spheroid MSCs in culture dishes, the MSCs were cultured in medium supplemented with or without BMP-2 (20 ng/ml, Pepro Tech. Inc., NJ, USA).

2.2. Generation of β-catenin knockout (*Ctnnb* KO) cell MSCs

We used CRISPR/Cas9 design tool with CRISPR/Cas9 vector (px330-U6-CBh- hSpCas9, Addgene, Cambridge, MA, USA) for genome editing. The vector was linearized by BbsI, and guide oligos were cloned into the vector using DNA ligase. The plasmids were transfected into the cells using Lipofectamine® 3000 (Thermo Fisher Sci., Tokyo, Japan). The next day, single cells were sorted into 96-well plates. After 2 weeks, colonies emerged, and single

colonies were expanded into 6-well plates. The *Ctnnb* KO cells and parent (WT) cells were selected using Western blot analysis.

2.3. RNA isolation and qRT-PCR

Total RNA was extracted from the cells using the TRIzol reagent. First-strand cDNA was synthesized from 3 μg total RNA using SuperScript II reverse transcriptase (Invitrogen, Thermo Fisher Scientific, MA, USA). To detect mRNA expression, we selected specific primers based on the nucleotide sequence of the resultant cDNA. The qRT-PCR analyses of targeted mRNAs were performed using SYBR Prime Script RT-PCR kit and Bio-Rad C system (Bio-Rad, Hercules, CA, USA). Reaction conditions were: an initial step at 95 °C for 30 s, followed by 40 cycles of denaturation at 95 °C for 5 s, annealing at 60 °C for 10 s and extension at 72 °C for 35 s. The threshold cycle (Ct) was defined as the fractional cycle number. The gene expression level was expressed relative to that of GAPDH that provides an internal standard for the amount of RNA isolated from a specimen. The delta (delta Ct) method was used to calculate the fold change for each sample. The relative Ct was normalized by the value before BMP-2 (day0).

2.4. Western blot analysis

Cells were then lysed in TNT buffer (Roche, Basel, Switzerland). The protein content was measured using a protein assay kit (Pierce, Hercules, CA, USA). Twenty micrograms proteins were subjected to 10% sodium dodecyl sulfate polyacrylamide gel electrophoresis, and the separated proteins were electrophoretically transferred to a polyvinylidene fluoride membrane at 75 V and 4°C for 1.5 h. The membrane was incubated with the targeted and internal control antibodies in 5% skim milk TBST (10 mM tris-HCl, 50 mM, NaCl 0.25% Tween-20) overnight at 4 °C. The blots were washed in TBST and incubated for 1 h with

horseradish peroxidase conjugated secondary antibodies in 5% skim milk TBST and developed using chemiluminescent system (GE Healthcare, Tokyo, Japan). The signal intensity of chemiluminescence was quantitatively analyzed with ImageJ software (NIH, Bethesda, MD).

2.5. Transplantation of 2D or 3D spheroid MSCs into calvarial bone defect model mice

Animal studies were conducted in accordance with the protocols approved by the Animal Care and Use Committee of Fukuoka Dental College (No. 17025). All surgeries were performed under general anesthesia induced 2% isoflurane using an air mixture gas machine (SF-B01, MR Technology, Inc., Ibaraki, Japan). A circular bone defect (4 mm diameter) was created in the calvarial bone with a trephine drill. Controls transplanted with a collagen sponge (CS; Zimmer Biomet Holdings, Inc., Warsaw, USA). The mice were divided into three groups: (a) control, (b) transplated 2D MSCs and CS (c) transplated 3D spheroid MSCs and CS. Some experiments, *Ctnnb* KO cells instead of wild type cells transplanted into calvarial bone defects.

2.6. Microcomputed tomography analysis

Microcomputed tomography (μ-CT) images were taken using μ-CT equipment (Skyscan-1176; Bruker, Belgium). The percentage of new bone formation was calculated from each μ-CT image as the area of new formed bone/area of the original defect, in accordance with our previous paper [11]. The percentage of new bone formation in the defect (% of new bone) was calculated as the total area of new bone formation per 5 μ-CT images × 100.

2.7. Statistical analyses

Data are expressed as the mean ± standard error of the mean (SEM). Differences were analyzed by one-way analysis of variance and Scheffe's multiple comparison tests.
P-values < 0.05 were considered to be significant.

3. Results

3.1. Expression of stemness-associated genes was upregulated in the 3D spheroid MSC and decreased during osteogenesis

First, we conducted mRNAs in 3D spheroid MSCs and compared them with those in 2D monolayer MSCs during osteogenesis. Quantitative reverse transcription polymerase chain reaction analysis showed that the basal expression levels of stemness-associated genes, such as *Nanog*, *Oct4*, *Klf4* and *Sox2* mRNAs, were also upregulated in the culture of 3D spheroid MSCs without BMP-2 treatment compared with those in the 2D monolayer MSCs (Fig. 1A). BMP-2 significantly downregulated the stemness-related genes in the 3D spheroid MSCs in a time-dependent manner but remained constant or was slightly increased on these genes in 2D monolayer MSCs, which was consistent with DNA microarray data (Fig. 1B). The culture of 3D spheroid MSCs also upregulated the expression of OCT4A and Nanog proteins compared with the 2D monolayers MSCs, and BMP-2 downregulated these in 3D spheroid MSCs but had little effect on them in 2D monolayer MSCs.

3.2. BMP-2 significantly upregulated the expression of osteogenesis-related molecules in 3D spheroid MSCs compared with that in 2D monolayer MSCs

BMP-2 increased the expression of osteogenesis-related genes, such as *ALP*, *Runx2*, and *OSX* mRNAs, compared with those in the control (without BMP-2) in both types of culture (Fig. 1C). The expression of their mRNAs and proteins after BMP-2 treatment was significantly upregulated in 3D spheroid MSCs in a time-dependent manner compared with

that in 2D monolayer MSCs (Fig. 1C and Fig. 2A). The peak time for expression of mRNAs after BMP-2 treatment was 5 d in 2D monolayer MSCs and 3 d in 3D spheroid MSCs. Furthermore, BMP-2 significantly activated its downstream molecules, such as p-Smad1/5, p-p38, and p-ERK, in 3D spheroid MSCs compared with those in 2D monolayer MSCs (Fig. 2A).

3.3. BMP-2 simultaneously induced Wnt/β-catenin and Hippo-associated molecules in the 3D spheroid MSC culture

BMP-2 transiently upregulated the expression of β-catenin mRNAs and proteins, and its expression was significantly increased in 3D spheroid MSCs than in 2D MSCs during osteogenesis (Fig. 1D and Fig. 2B). Similar results were obtained after being stimulated with osteogenesis-induced medium. Furthermore, the upregulation of GSK3-β, a β-catenin suppressor, conversely decreased the expression of β-catenin proteins after BMP-2 treatment in both types of culture (Fig. 2B). Transcriptional coactivator YAP and transcriptional coactivator with PDZ-binding motif (TAZ) and Hippo-signaling molecules have recently been implicated as regulators of osteoblast differentiation [12-14]. To clarify whether 3D spheroid MSCs activate YAP/TAZ during osteogenesis, we examined the effect of BMP-2 treatment on the expression of YAP/TAZ in 3D spheroid MSCs in the present experiments. BMP-2 transiently downregulated YAP/TAZ expression on day 1 and then upregulated it more in 3D spheroid MSCs than in 2D monolayer MSCs. Furthermore, to determine whether these transcriptional factors localize to the nucleus during osteogenesis in 3D spheroid MSCs, we examined the expression of their proteins on nuclear proteins after BMP-2 treatment (Fig. 2C). The translocation of β-catenin and YAP/TAZ, as well as p-Smad 1/5/9, significantly increased in 3D spheroid MSCs compared with those in 2D MSCs.

3.4. BMP-2 did not induce osteogenesis and bone regeneration in β-catenin knockout 3D spheroid MSCs

To clarify the potential role of Wnt/β-catenin and its related molecules that were activated in 3D spheroid MSCs during osteogenesis, we generated KO MSCs targeted to β-catenin (*Ctnnb* KO MSCs) using the CRISP/Cas9 vector. Expression of only β-catenin protein but not the other osteogenesis- and Hippo-related proteins was effectively inhibited in *Ctnnb* KO MSCs compared with those in the parent MSCs (Fig. 3A and Supplemental Fig. 1). BMP-2-induced upregulation of the osteogenesis-related mRNAs and proteins in 2D monolayer *Ctnnb* KO MSCs was similar to that of parent WT 2D monolayer MSCs (Fig. 3A and Fig. 3B); however, BMP-2 had nearly no effect on osteogenesis-related mRNAs and proteins in 3D spheroid *Ctnnb* KO MSCs. In addition, the nuclear translocation of osteogenesis-related molecules was partially suppressed in 3D spheroid *Ctnnb1* KO MSCs, but not in 2D monolayer *Ctnnb* KO MSCs (Fig. 3C).

3.5. Implantation with 3D spheroid MSCs promoted new bone formation in aged mice with a calvarial defect

To clarify whether 3D spheroid MSCs could potentiate new bone formation more than 2D monolayer MSCs *in vitro*, we transplanted a collagen sponge scaffold (control) with 3D spheroid MSCs or 2D monolayer MSCs into 40-week-old mice with a calvarial bone defect (Fig. 4A). Previous reports, including ours, have suggested that calvarial defects in mice >30 weeks old do not heal spontaneously during bone regeneration [11, 15]. Two weeks after transplantation, μ-CT images revealed no difference in the mouse calvarial defects among the control, transplantation with 2D MSCs, and transplantation with 3D spheroid MSCs groups (Fig. 4A and Fig. 4B). Four weeks after transplantation, the small peninsulas of new bone formed in the MSC-transplanted mice with higher rates noted in the mice

transplanted with 3D spheroid transplantation than in the mice in the control or 2D transplantation groups. This trend continued for up to 12 weeks. Consistent with the data using μ-CT analysis, histological analysis of hematoxylin and eosin (HE)-stained sections showed that new bone regeneration significantly increased in mice transplanted with 3D spheroid MSCs compared with that in the control or 2D monolayer MSC groups 12 weeks after transplantation (Fig. 4C).

To clarify furthermore whether 3D spheroid *Ctnnb* KO MSCs suppress new bone formation, we transplanted a collagen sponge scaffold (control) with 3D spheroid *Ctnnb1* KO MSCs or 2D monolayer *Ctnnb* KO MSCs into 40-week-old mice with calvarial bone defects Surprisingly, μ-CT analysis and HE staining showed little new bone formation in the calvarial bone in any of the three types of transplantation, which indicated that the upregulation of β-catenin and its related molecules in 3D spheroid MSCs promoted bone regeneration in calvarial defects more than in 2D monolayer MSCs.

4. Discussion

3D spheroid MSC cultures have some advantages over the standard 2D monolayer MSC cultures. The 3D spheroid MSC culture allows the cells to adapt to their native shape, the upregulation of cell-to-cell contacts, and the interaction between the cells and the extracellular matrix [10, 16]. In the present experiments, we demonstrated three lines of evidence to support the conclusion that 3D spheroid MSCs enhance osteogenic potential and promote bone regeneration compared with 2D monolayer MSCs as follows: 1) 3D spheroid MSCs exhibited increased stemness molecules, 2) the expression of osteogenesis-related molecules was upregulated in 3D spheroid MSCs together with the activation of Wnt/β-catenin signaling, and 3) new bone regeneration was activated after transplanting WT 3D

spheroid MSCs into the bone defect model mice but little was activated after transplanting *Ctnnb* (β-catenin) KO spheroid MSCs.

The culture of 3D spheroid MSCs enhanced the expression of other desirable phenotypes, such as improved MSC stemness and increased survival after transplantation [6]. MSCs retain their physiological behaviour longer in cultures of 3D spheroid MSCs compared with that of 2D monolayer MSCs [17]. The transplantation of 3D spheroid MSCs into animals induces these cells to differentiate into the tissues that are nearly indistinguishable from those of native organs [18].

In our *in vitro* experiments, the 3D spheroid MSCs was upregulated stemness marker expression, and the osteogenesis differentiation capacity was higher than that in 2D monolayer MSCs. Moreover, the transplantation of 3D spheroid MSCs, but not 3D spheroid *Ctnnb KO MSCs, in vivo* promoted new bone formation in the calvarial defect in aged mice, which suggested a key pathway in 3D-activated Wnt/β-catenin signaling.

Wnt signalling is known as a major developmental signalling pathway that is particularly critical in stem cell maintenance and differentiation; however, no Wnt signalling activation was detected during osteogenic differentiation in 2D monolayer hTERT MSCs, which indicated that active Wnt signalling is not a biological requirement in 2D monolayer MSCs [19]. Furthermore, Wnt signalling has been reported to distinctively regulate MSCs in a biphasic manner, exhibiting proliferation and self-renewal under low Wnt/β-catenin signalling and enhancement of osteoblastogenesis with priming to osteoblast lineages under high Wnt/β-catenin signalling [20]. In the present study, the environment of the 3D spheroid MSC culture is more closely recaptured in very simplistic terms *in vivo*, which activates Wnt/β-catenin signalling in 3D spheroid MSCs compared with that in 2D monolayer MSCs. In contrast, BMP-2 induces p-Smad1/5 nuclear translocation in both 3D spheroid *Ctnnb* KO MSCs. Similar results were observed in the present *in vivo* experiments by transplanting 3D

spheroid MSCs into the calvarial defect mouse model. These findings indicated that the culture of 3D spheroid MSCs activated Wnt/β-catenin as well as Smad signalling, which resulted in synergistic osteogenesis effects on bone regeneration *in vivo*.

On the other hand, MSCs have been reported to express several different secretomes during 3D spheroid MSC culture, such as increased wound-healing features and angiogenesis cytokines [21, 22]. MSCs must be primed with proinflammatory cytokines to acquire their anti-inflammatory properties [23, 24], and spheroid MSCs are self-stimulated by autocrine interleukin-1 signalling to have enhanced anti-inflammatory effects [25]. Furthermore, 3D spheroid MSCs were upregulated the expression of CXCR4 [26, 27], resulting in restore cell adhesion and nitche area to stem cell homing. We found that the ability of osteoblastogenesis is higher in 3D spheroid MSCs than in 2D MSCs in vitro present experiments. Furthermore, the small peninsulas of new bone were formed in around centre of the defect in the MSC-transplanted mice, suggesting the transplanted MSCs kept in the defect area and differentiated into osteoblastic lineage. The calvarial bone repairs are suggested to cause by not only promotion in some released regulator factors but also promotion in osteoblastic differentiation from 3D spheroid MSCs.

Interestingly, the high activation of Wnt/β-catenin pathways in 3D spheroid MSCs in the current study was characterized by the promotion of bone formation with osteoblast differentiation. Namely, the upregulation of β-catenin in 3D spheroid MSCs is caused by the promotion of new bone formation that is not observed in 2D monolayer MSCs. Wnt10b transgenic mice have been reported to have increased bone mass with Wnt10b in osteoblasts from the osteocalcin promoter [28], led to the identification of Wnt10b as a stimulator [29]. These findings suggest that the Wnt10b secreted from 3D spheroid MSCs are self-activated by Wnt/β-catenin and its downstream pathways in an autocrine mode, which results in enhanced differentiation into osteoblast lineages.

YAP/TAZ molecules have recently been recognized as key factors in mechanotransduction and cell polarity [30-33] when activated together with Runx2 and Smads in MSCs during osteogenesis [13, 14]. The recruitment of TAZ to Runx2 target genes has been reported to enhance the osteogenic transcriptional process [34]. TAZ knockdown in bone marrow MSCs led to an absence of calcium deposition. On the other hand, the BMP-2 in the present experiments transiently downregulated the expression of TAZ in 3D spheroid MSCs and then upregulated it during osteoblastogenesis, resulting in differentiation of osteoblast lineages differentiated from 3D spheroid *Ctnnb* KO MSCs. Similar to these data, it has been reported that YAP/TAZ in osteoblast progenitors play a negative role in regulating osteoblastogenesis, indicating that YAP/TAZ has opposite effects at different stages during osteoblastogenesis.

There are various approaches to improve MSC efficiency, and 3D spheroid MSCs have advantages in optimal therapeutic protocols. MSCs derived from osteoporosis patients exhibit low proliferating and differentiating activity during osteogenesis [35]. These results suggest the need for alternative cell characteristics that can be easily prepared and expanded, especially in elderly patients with metabolic disorders; therefore, to acquire more effective bone-regenerative therapy, it is suggested that these patients be transplanted autologous 3D spheroid MSCs in their constitutive active form for Wnt/β-catenin signaling.

Funding

This work was supported by Grants-in-Aid for Scientific Research from the Ministry of Education, Culture, Sports, Science and Technology of Japan (15K11062 to HK) and the Private University Research Branding Project at Fukuoka Dental College.

References

1. A. Aldahmash, W. Zaher, M. Al-Nbaheen, Human stromal (mesenchymal) stem cells: basic biology and current clinical use for tissue regeneration, Ann Saudi Med. 32 (2012) 68-77. https://doi.org/10.5144/0256-4947.2012.68.
2. Z.Y. Zhang, S.H. Teoh, J.H. Hui, The potential of human fetal mesenchymal stem cells for off-the-shelf bone tissue engineering application, Biomaterials. 33 (2012) 2656-2672. https://doi.org/10.1016/j.biomaterials.2011.12.025.
3. K. Takahashi, S. Yamanaka, Induction of pluripotent stem cells from mouse embryonic and adult fibroblast cultures by defined factors, Cell. 126 (2006) 663-676. https://doi.org/10.1016/j.cell.2006.07.024.
4. P.A. Zuk, M. Zhu, H. Mizuno, Multilineage cells from human adipose tissue: implications for cell-based therapies, Tissue Eng. 7 (2001) 211-228. https://doi.org/10.1089/107632701300062859.
5. G.S. Huang, C.S. Tseng, Yen. B. Linju, Solid freeform-fabricated scaffolds designed to carry multicellular mesenchymal stem cell spheroids for cartilage regeneration, Eur Cell Mater. 26 (2013) 179-194. DOI: 10.22203/eCM.v026a13.
6. Z. Cesarz, K. Tamama, Spheroid Culture of Mesenchymal Stem Cells, Stem Cells Int. (2016). http://dx.doi.org/10.1155/2016/9176357.
7. S. Sart, T. Ma, Y. Li, Extracellular matrices decellularized from embryonic stem cells maintained their structure and signalling specificity, Tissue Eng Part A. 20(2014) 54-66. https://doi.org/10.1089/ten.tea.2012.0690.
8. M. Ader, E.M. Tanaka, Modeling human development in 3D culture, Curr Opin Cell Biol. 31 (2014) 23-28. https://doi.org/10.1016/j.ceb.2014.06.013.

9. T.J. Bartosh, J.H. Ylöstalo, A. Mohammadipoor, Aggregation of human mesenchymal stromal cells (MSCs) into 3D spheroids enhances their antiinflammatory properties, Proc Natl Acad Sci U S A. 107 (2010) 1324-1329. https://doi.org/10.1073/pnas.1008117107.

10. W. Wang, K. Itaka, S. Ohba, 3D spheroid culture system on micropatterned substrates for improved differentiation efficiency of multipotent mesenchymal stem cells, Biomaterials. 30 (2009) 2705-2715. https://doi.org/10.1016/j.biomaterials.2009.01.030.

11. Y. Katsumata, H. Kajiya, K. Okabe, A salmon DNA scaffold promotes osteogenesis through activation of sodium-dependent phosphate cotransporters, Biochem Biophys Res Commun. 468 (2015) 622-628. https://doi.org/10.1016/j.bbrc.2015.10.172.

12. L. Azzolin, F. Zanconato, S. Bresolin, Role of TAZ as mediator of Wnt signaling, Cell. 151 (2012) 1443-1456. https://doi.org/10.1016/j.cell.2012.11.027.

13. T.A. Beyer, A. Weiss, Y. Khomchuk, Beyer Switch enhancers interpret TGF-β and Hippo signaling to control cell fate in human embryonic stem cells, Cell Rep. 5 (2013) 1611-1624. https://doi.org/10.1016/j.celrep.2013.11.021.

14. M.R. Byun, J.H. Hwang, A.R. Kim, Canonical Wnt signaling activates TAZ through PP1A during osteogenic differentiation, Cell Death Differ. 21 (2014) 854-863. https://doi.org/10.1038/cdd.2014.8.

15. B. Levi, M.T. Longaker, Concise review: adipose-derived stromal cells for skeletal regenerative medicine, Stem Cells. 29 (2011) 576-582. https://doi.org/10.1002/stem.612.

16. S.K. Kapur, X. Wang, H. Shang, Human adipose stem cells maintain proliferative, synthetic and multipotential properties when suspension cultured as self-assembling spheroids, Biofabrication. 4 (2012) https://doi.org/10.1088/1758-5082/4/2/025004.

17. M. Caiazzo, Y. Okawa, A. Ranga, Defined three-dimensional microenvironments boost induction of pluripotency, Nat Mater. 15 (2016) 344-352. https://doi.org/10.1038/nmat4536

18. A. Peloso, A. Dhal, J.P. Zambon, Current achievements and future perspectives in whole-organ bioengineering, Stem Cell Res Ther. 6 (2015) https://doi.org/10.1186/s13287-015-0089-y

19. S. James, J. Fox, F. Afsari, Multiparameter Analysis of Human Bone Marrow Stromal Cells Identifies Distinct Immunomodulatory and Differentiation-Competent Subtypes, Stem Cell Reports. 4 (2015) 1004-1015. https://doi.org/10.1016/j.stemcr.2015.05.005.

20. J.A. Kim, H.K. Choi, T.M. Kim, Regulation of mesenchymal stromal cells through fine tuning of canonical Wnt signaling, Stem Cell Res. 14 (2015). https://doi.org/10.1016/j.scr.2015.02.007.

21. S.H. Bhang, S. Lee, T.J. Lee , Three-dimensional cell grafting enhances the angiogenic efficacy of human umbilical vein endothelial cells, Tissue Eng Part A. 18 (2012). https://doi.org/10.1089/ten.tea.2011.0193.

22. L. Guo, J. Ge, Y. Zhou, Three-dimensional spheroid-cultured mesenchymal stem cells devoid of embolism attenuate brain stroke injury after intra-arterial injection, Stem Cells Dev. 23 (2014) 978-989. https://doi.org/10.1089/scd.2013.0338.

23. K. English, A. French, K.J. Wood, Mesenchymal stromal cells: facilitators of successful transplantation?, Cell Stem Cell. 7 (2010) 431-442. https://doi.org/10.1016/j.stem.2010.09.009.

24. Y. Shi, J. Su, A. Robert, How mesenchymal stem cells interact with tissue immune responses, Trends Immunol. 33 (2012) 136-143. https://doi.org/10.1016/j.it.2011.11.004.

25. T.J. Bartosh, J.H. Ylöstalo, N. Bazhanov, Dynamic compaction of human mesenchymal stem/precursor cells into spheres self-activates caspase-dependent IL1 signaling to enhance secretion of modulators of inflammation and immunity (PGE2, TSG6, and STC1), Stem Cells. 31 (2013) 2443-2456. https://doi.org/10.1002/stem.1499.

26. Z. Cesarz, J.L. Funnell, J. Guan, Soft elasticity-associated signaling and bone morphogenic protein 2 are key regulators of mesenchymal stem cell spheroidal aggregates, Stem Cells Dev. 25 (2016) 622-635. https://doi.org/10.1089/scd.2015.0356.

27. I.A. Potapova, P.R. Brink, I.S. Cohen, Culturing of human mesenchymal stem cells as three-dimensional aggregates induces functional expression of CXCR4 that regulates adhesion to endothelial cells, J Biol Chem. 283 (2008) 13100-13107. https://doi.org/10.1074/jbc.M800184200.

28. C.N. Bennett, H. Ouyang, Y.L. Ma, Wnt10b increases postnatal bone formation by enhancing osteoblast differentiation, J Bone Miner Res. 22 (2007) 1924-1932. https://doi.org/10.1359/jbmr.070810.

29. S. Kang, C.N. Bennett, I. Gerin, Wnt signaling stimulates osteoblastogenesis of mesenchymal precursors by suppressing CCAAT/enhancer-binding protein alpha and peroxisome proliferator-activated receptor gamma, J Biol Chem. 282 (2007) 14515-14524. DOI:10.1074/jbc.M700030200.

30. S.E. Ross, N. Hemati, K.A. Longo, Inhibition of adipogenesis by Wnt signaling, Science. 289 (2000) 950-953. DOI:10.1126/science.289.5481.950.

31. G. Halder, S. Dupont, S. Piccolo, Transduction of mechanical and cytoskeletal cues by YAP and TAZ, Nat Rev Mol Cell Biol. 13 (2012) 591-600. DOI:10.1038/nrm3416.

32. T. Panciera, L. Azzolin, M. Cordenonsi, Mechanobiology of YAP and TAZ in physiology and disease, Nat Rev Mol Cell Biol. 18 (2017) 757-770. DOI:10.1038/nrm.2017.87

33. K. Wada, K. Itoga, T. Okano, Hippo pathway regulation by cell morphology and stress fibers, Development. 138 (2011) 3907-3914. DOI:10.1242/dev.070987.

34. J.H. Hong, E.S. Hwang, M.T. McManus, TAZ, a transcriptional modulator of mesenchymal stem cell differentiation, Science. 309 (2005) 1074-1078. DOI:10.1126 / science.1110955.

35. J.P. Rodríguez, S. Ríos, M. Fernández, Differential activation of ERK1, 2 MAP kinase signaling pathway in mesenchymal stem cell from control and osteoporotic postmenopausal women, J Cell Biochem, 92 (2004) 745-754 DOI:10.1002/jcb.20119

Figure legends

Fig 1. 3D MSC formation rapidly increases stemness markers, and BMP-2 significantly upregulated the expression of osteogenesis and *Wnt/beta-catenin* markers.

Basal and BMP-2 induced expression of stemness (A and B), osteogenesis, and Wnt/beta-catenin genes using 2D MSC or 3D MSC cultures. Data shown are mean ± SEM. ** indicates $p < 0.05$ and $p < 0.01$ vs. day 0 (before BMP-2 treatment). The relative level of protein expression was normalized by the value before BMP-2 treatment (day 0).

Fig. 2. The 3D MSC simultaneously upregulated the expression of *Wnt/beta-catenin* and *Hippo*-signaling molecules.

Treatment with BMP-2 was analyzed total proteins (A and B) or their nuclear proteins(C) by Western blotting and normalized to internal control.

Fig.3. BMP-2 induced little osteogenesis in 3D spheroid *Ctnnb* KO MSCs.

Treatment with BMP-2 was analyzed total proteins (A and B) or their nuclear proteins(C) in Ctnnb KO 2D and 3D MSC by Western blotting and normalized to internal control.

Fig. 4. Transplantation with 3D and 2D WT and *Ctnb* KOMSCs induced little bone repair with calvarial bone defects.

(A and B) Micro-CT images of implantation at 2, 4, 8, and 12 weeks after surgery in 40-week-old mice. (C) Histological calvarial tissues at 12 weeks after surgery. B and N indicate the original and new bone, respectively; C indicates connective tissues. Scale bar represents 500 μm.

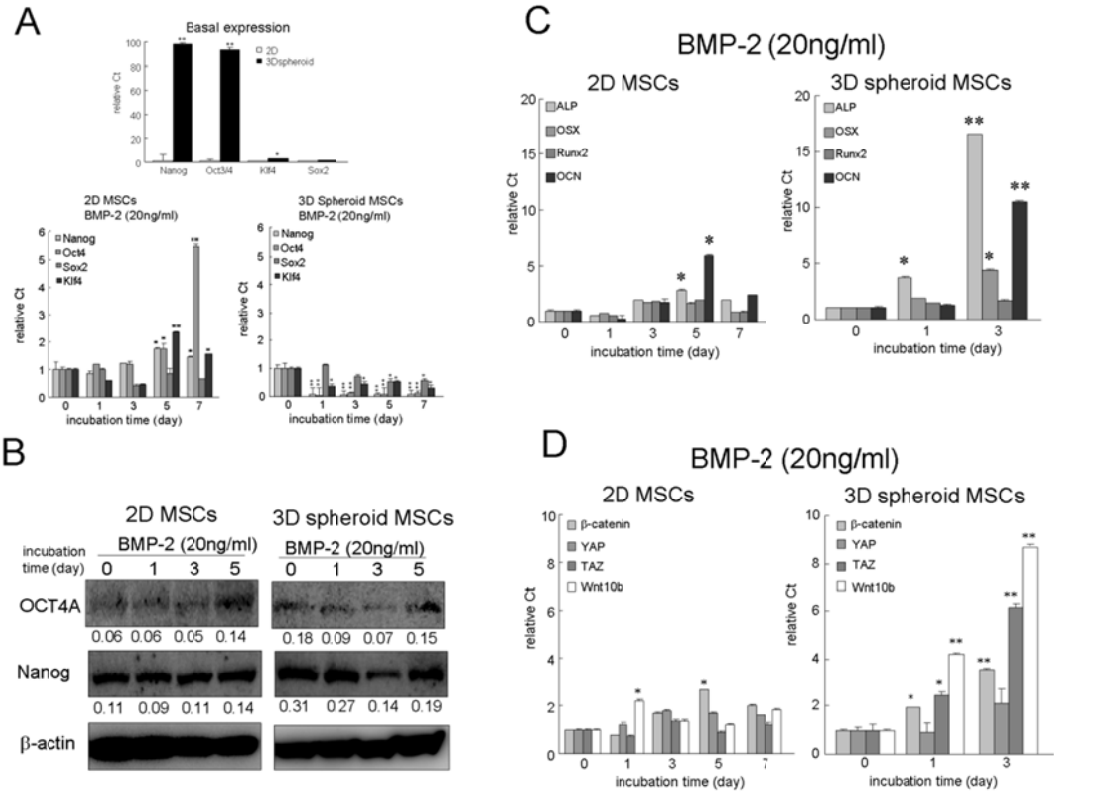
A
Easal expression
2D
3Dspheroid
relative Ct
Nanog
Oct3/4
Klf4
Sox2
2D MSCs
BMP-2 (20ng/ml)
3D Spheroid MSCs
BMP-2 (20ng/ml)
Nanog
Oct4
Sox2
Klf4
incubation time (day)
C
BMP-2 (20ng/ml)
2D MSCs
3D spheroid MSCs
ALP
OSX
Runx2
OCN
relative Ct
incubation time (day)
B
2D MSCs
3D spheroid MSCs
BMP-2 (20ng/ml)
incubation time (day)
OCT4A
Nanog
β-actin
0.06 0.06 0.05 0.14
0.18 0.09 0.07 0.15
0.11 0.09 0.11 0.14
0.31 0.27 0.14 0.19
D
BMP-2 (20ng/ml)
2D MSCs
3D spheroid MSCs
β-catenin
YAP
TAZ
Wnt10b
relative Ct
incubation time (day)

Fig. 1

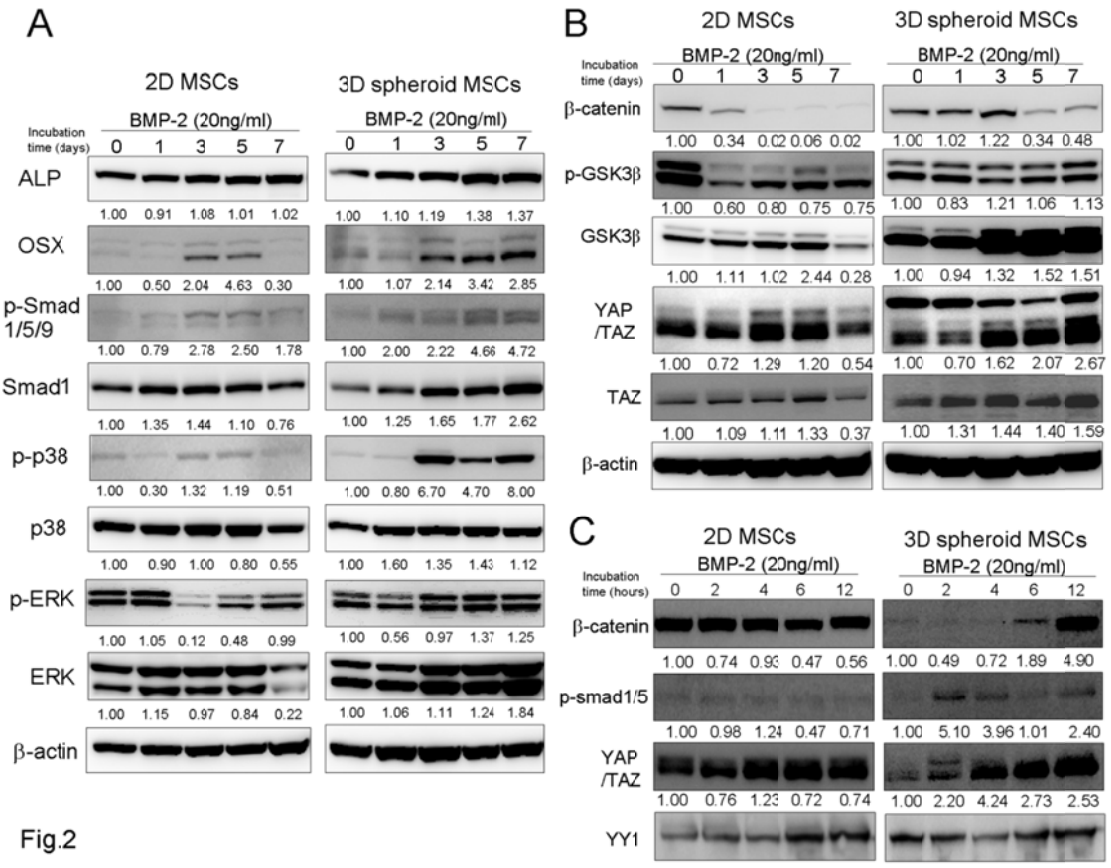
A
2D MSCs
3D spheroid MSCs
BMP-2 (20ng/ml)
Incubation time (days)
0 1 3 5 7
ALP
1.00 0.91 1.08 1.01 1.02
1.00 1.10 1.19 1.38 1.37
OSX
1.00 0.50 2.04 4.63 0.30
1.00 1.07 2.14 3.42 2.85
p-Smad 1/5/9
1.00 0.79 2.78 2.50 1.78
1.00 2.00 2.22 4.66 4.72
Smad1
1.00 1.35 1.44 1.10 0.76
1.00 1.25 1.65 1.77 2.62
p-p38
1.00 0.30 1.32 1.19 0.51
1.00 0.80 6.70 4.70 8.00
p38
1.00 0.90 1.00 0.80 0.55
1.00 1.60 1.35 1.43 1.12
p-ERK
1.00 1.05 0.12 0.48 0.99
1.00 0.56 0.97 1.37 1.25
ERK
1.00 1.15 0.97 0.84 0.22
1.00 1.06 1.11 1.24 1.84
β-actin
B
2D MSCs
3D spheroid MSCs
BMP-2 (20ng/ml)
Incubation time (days)
0 1 3 5 7
β-catenin
1.00 0.34 0.02 0.06 0.02
1.00 1.02 1.22 0.34 0.48
p-GSK3β
1.00 0.60 0.80 0.75 0.75
1.00 0.83 1.21 1.06 1.13
GSK3β
1.00 1.11 1.02 2.44 0.28
1.00 0.94 1.32 1.52 1.51
YAP /TAZ
1.00 0.72 1.29 1.20 0.54
1.00 0.70 1.62 2.07 2.67
TAZ
1.00 1.09 1.11 1.33 0.37
1.00 1.31 1.44 1.40 1.59
β-actin
C
2D MSCs
3D spheroid MSCs
BMP-2 (20ng/ml)
Incubation time (hours)
0 2 4 6 12
β-catenin
1.00 0.74 0.93 0.47 0.56
1.00 0.49 0.72 1.89 4.90
p-smad1/5
1.00 0.98 1.24 0.47 0.71
1.00 5.10 3.96 1.01 2.40
YAP /TAZ
1.00 0.76 1.23 0.72 0.74
1.00 2.20 4.24 2.73 2.53
YY1

Fig.2

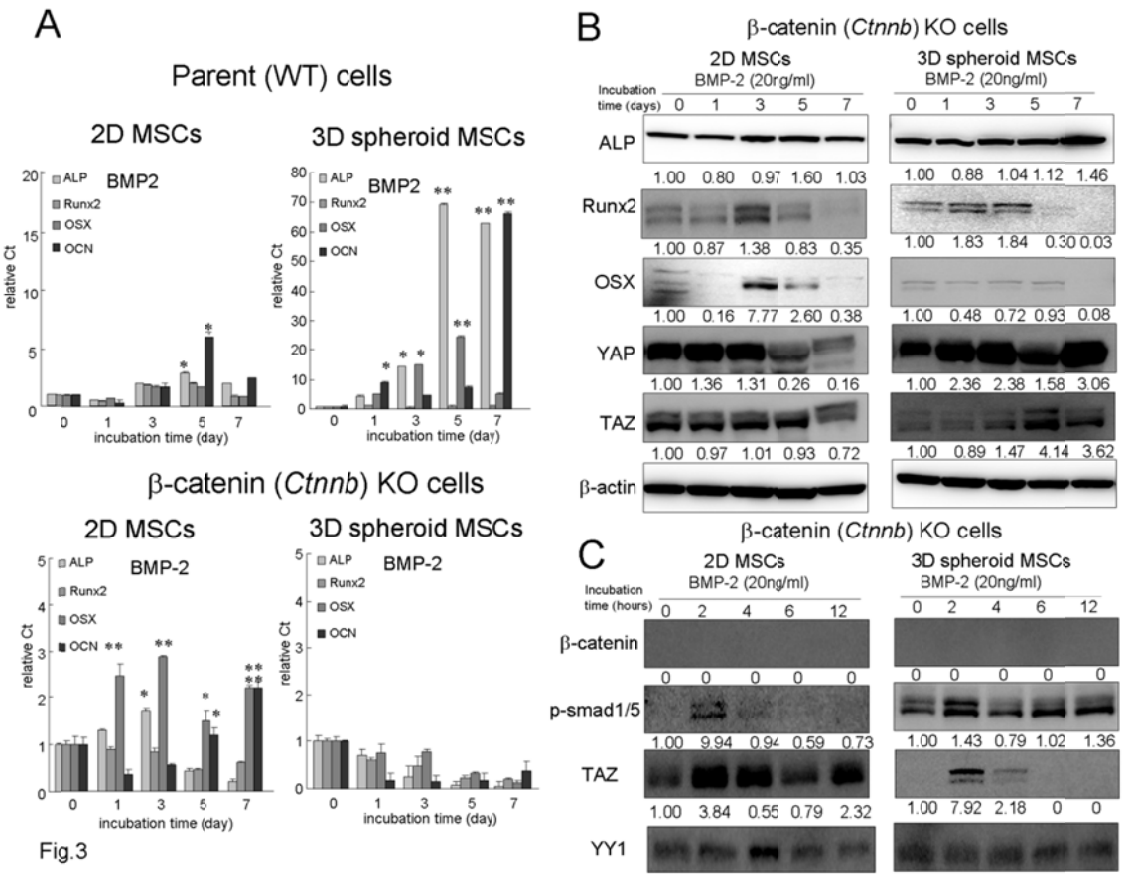
A
Parent (WT) cells
2D MSCs
3D spheroid MSCs
ALP
Runx2
OSX
OCN
BMP2
relative Ct
incubation time (day)
β-catenin (Ctnnb) KO cells
BMP-2
B
β-catenin (Ctnnb) KO cells
2D MSCs
3D spheroid MSCs
BMP-2 (20rg/ml)
BMP-2 (20ng/ml)
Incubation time (days)
ALP
Runx2
OSX
YAP
TAZ
β-actin
C
β-catenin (Ctnnb) KO cells
Incubation time (hours)
β-catenin
p-smad1/5
TAZ
YY1

Fig.3

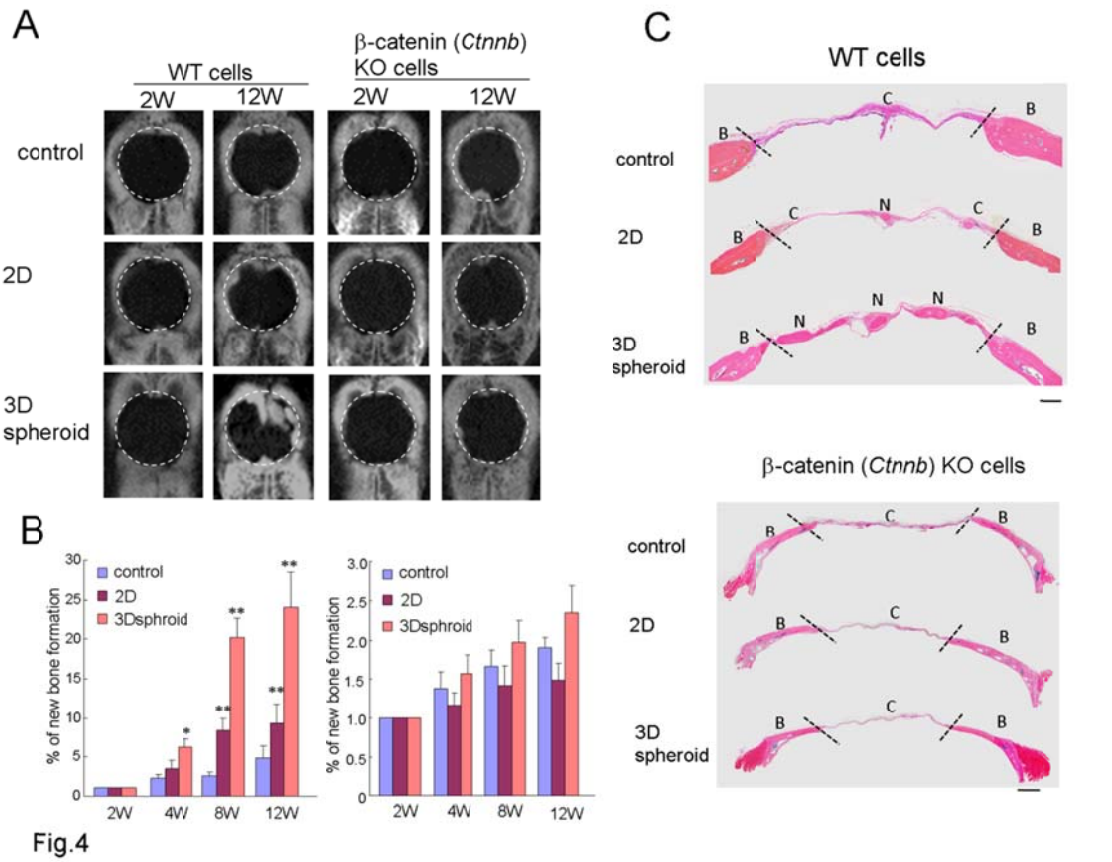
A
WT cells
β-catenin (Ctnnb) KO cells
2W
12W
control
2D
3D spheroid
B
control
2D
3Dsphroid
% of new bone formation
2W
4W
8W
12W
C
WT cells
control
2D
3D spheroid
β-catenin (Ctnnb) KO cells
B
C
N

Fig.4

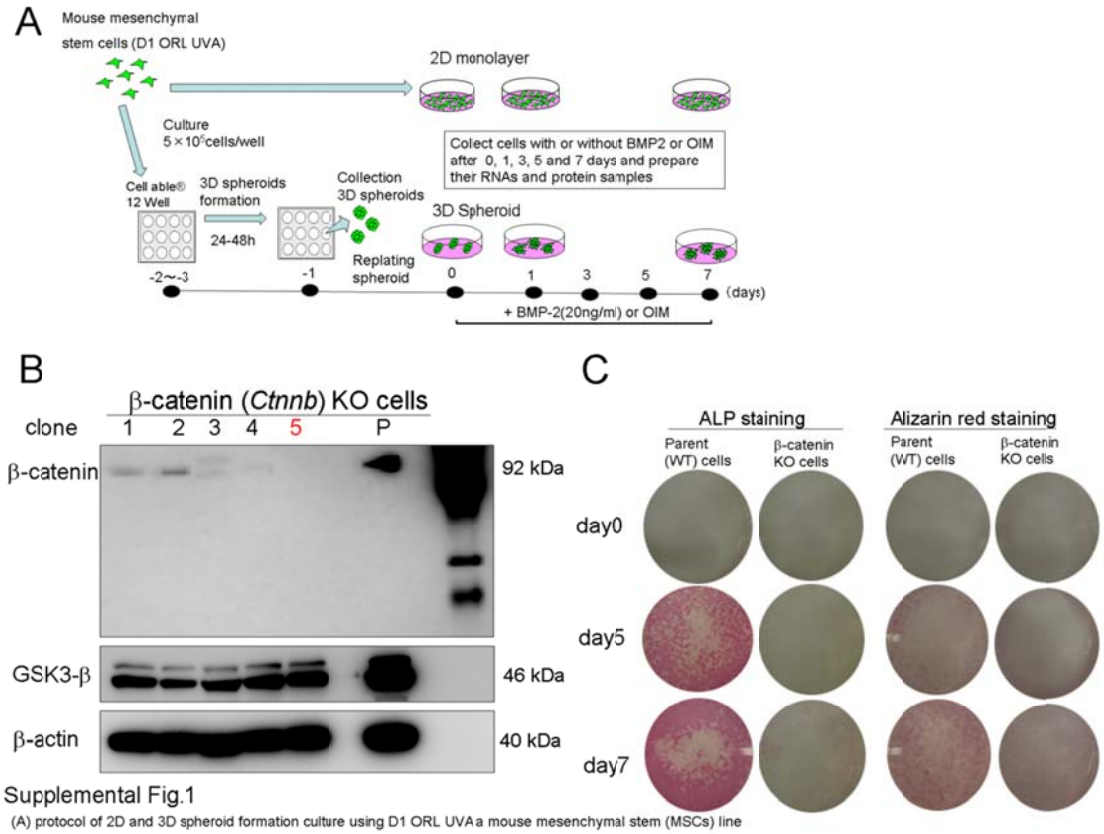

Supplemental Fig.1

(A) protocol of 2D and 3D spheroid formation culture using D1 ORL UVA a mouse mesenchymal stem (MSCs) line

(B) Construction and selection of β-catenin (*Ctnnb*) KO MSCs

(C) ALP and Alizarin red staining in parents (WT) and β-catenin (*Ctnnb*) KO during osteogenesis